



HAL
open science

A heteroleptic diradical Cr(III) complex with extended spin delocalization and large intramolecular magnetic exchange

Xiaozhou Ma, Elizaveta Suturina, Mathieu Rouzières, Fabrice Wilhelm, Andrei Rogalev, Rodolphe Clérac, Pierre Dechambenoit

► **To cite this version:**

Xiaozhou Ma, Elizaveta Suturina, Mathieu Rouzières, Fabrice Wilhelm, Andrei Rogalev, et al.. A heteroleptic diradical Cr(III) complex with extended spin delocalization and large intramolecular magnetic exchange. *Chemical Communications*, 2020, 56 (36), pp.4906-4909. 10.1039/d0cc00548g . hal-02877510

HAL Id: hal-02877510




<https://hal.science/hal-02877510>

Submitted on 24 Nov 2020

HAL is a multi-disciplinary open access archive for the deposit and dissemination of scientific research documents, whether they are published or not. The documents may come from teaching and research institutions in France or abroad, or from public or private research centers.

L'archive ouverte pluridisciplinaire **HAL**, est destinée au dépôt et à la diffusion de documents scientifiques de niveau recherche, publiés ou non, émanant des établissements d'enseignement et de recherche français ou étrangers, des laboratoires publics ou privés.

A heteroleptic diradical Cr(III) complex with extended spin delocalization and large intramolecular magnetic exchange†

Xiaozhou Ma,^a Elizaveta A. Sutura, ^b Mathieu Rouzières,^a Fabrice Wilhelm,^c Andrei Rogalev,^c Rodolphe Clérac ^{*a} and Pierre Dechambenoit ^{*a}

Successive chemical reductions of the heteroleptic complex [(tpy)-Cr^{III}(tphz)]³⁺ (tpy = terpyridine; tphz = tetrapyridophenazine) give rise to the mono- and di-radical redox isomers, [(tpy)Cr^{III}(tphz^{•-})]²⁺ and [(tpy^{•-})Cr^{III}(tphz^{•-})]⁺, respectively. As designed, the optimized overlap of the involved magnetic orbitals leads to extremely strong magnetic interactions between the $S = 3/2$ metal ion and $S = 1/2$ radical spins, affording well isolated $S_T = 1$ and $S_T = 1/2$ ground states at room temperature.

Extended spin delocalization in molecule-based materials is an attractive feature for spintronics¹ and for the design of permanent magnets.² This situation can be promoted using aromatic radicals, where unpaired electrons can be delocalized all over the π system. However, such a delocalization is usually much less marked when involving metal ions in coordination compounds, due to the symmetry and the relative orientations of the metal/ligand orbitals. This apparent problem can be bypassed by combining both magnetic metal ions and radical ligands in a single material and stabilizing strong magnetic exchange interactions between their spins,^{3,4} which are strongly dependent on the overlap of their singly occupied orbitals.⁴

Recently, our group designed a series of dinuclear complexes based on Co(II) and Ni(II) metal ions and redox-active tetrapyridophenazine (tphz)⁵ as the bridging ligand, for which radical forms are accessible and particularly stable.^{6,7} The magnetic interactions within the complexes can be tuned by successive reduction processes localized on the tphz ligand. Considering the particular tphz geometry and the z-axis orientation along the N

atoms of its pyridine groups, the d_{xy} orbital of a transition metal ion overlaps the best with the π -system of the aromatic bridging ligand, providing an excellent pathway for electron and spin delocalization. When this d_{xy} orbital is singly occupied like in the high-spin $3d^7$ Co(II) complex,⁶ this configuration promotes dominating and massive antiferromagnetic Co-radical interactions (< -500 K; $-2J$ formalism). Conversely, when d_{xy} is fully occupied for the $3d^8$ Ni(II) analogue, the orthogonality of the singly occupied d orbitals ($d_{x^2-y^2}$ and d_{z^2}) with the $tphz^{\bullet-}$ π -system leads to dominating and very strong ferromagnetic Ni-radical interactions (+214 K).⁷ This comparison between Co(II) and Ni(II) complexes evidenced the pivotal role played by the d_{xy} orbital in the strength of the magnetic metal-radical coupling and its influence on the spin delocalization.^{6,7}

Based on these conclusions, the $3d^3$ chromium(III) metal ion appears to be the best spin carrier candidate for promoting the strongest metal-radical antiferromagnetic exchange. With Cr^{3+} in a pseudo-octahedral environment, all t_{2g} orbitals are singly occupied (Fig. S6, ESI[†]), which guarantee an optimized π -d overlap and thus an excellent electronic communication between the metal ions and the bridging ligand. Meanwhile, the empty e_g orbitals exclude the competing presence of ferromagnetic contributions to the exchange coupling as observed in the Co(II) and Ni(II) complexes due to the orthogonality of the singly occupied e_g orbitals and the bridging ligand SOMO.† As a consequence, only extremely large antiferromagnetic coupling is expected between Cr(III) and the $tphz^{\bullet-}$ radical spins.

To test this hypothesis and validate our synthetic strategy toward complexes with large intramolecular interactions, a novel series of Cr(III) complexes based on the redox-active tphz ligand is reported. The reaction of an equimolar mixture of $Cr(tpy)(CF_3SO_3)_3$ ⁸ and tphz in CH_3CN leads to $[Cr(tphz)(tpy)](CF_3SO_3)_3 \cdot Et_2O$ (**1**), a new mononuclear chromium complex. Orange needle-shape crystals of **1** were isolated after slow diffusion of Et_2O vapors (ESI[†]). As confirmed from single crystal X-ray diffraction data at 120 K (Fig. 1 and Table S1, ESI[†]), the Cr ion resides in an octahedral environment bonded to three nitrogen atoms from tphz and another three from tpy. The valence of the Cr metal ions is

^a Univ. Bordeaux, CNRS, Centre de Recherche Paul Pascal, UMR 5031, 33600 Pessac, France. E-mail: rodolphe.clerac@crpp.cnrs.fr, pierre.dechambenoit@crpp.cnrs.fr

^b Department of Chemistry, University of Bath, Claverton Down, Bath BA2 7AY, UK

^c ESRF-The European Synchrotron, 38043 Grenoble Cedex 9, France

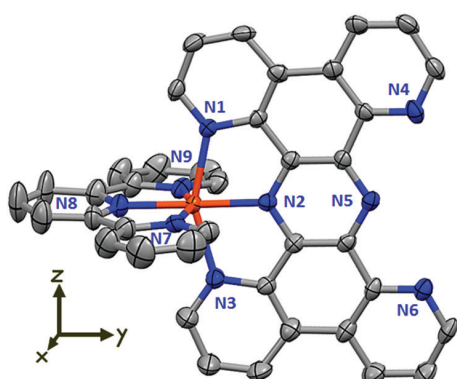


Fig. 1 Molecular structure of $[\text{Cr}(\text{tphz})(\text{tpy})]^{3+}$ in **1** at 120 K. Thermal ellipsoids are depicted at a 50% probability level. Grey: carbon; orange: chromium; blue: nitrogen. Hydrogen atoms, solvent molecules and counter anions are omitted for clarity. Note that the depicted Cartesian axes are not the crystallographic axes, but the orientation chosen for the denomination of the d orbitals.

consistent with a +3 oxidation state according to the bond valence sum calculation⁹ and by comparison of the Cr–N bond lengths (Table 1) with similar complexes^{10–12} and with the starting material $\text{Cr}^{\text{III}}(\text{tpy})(\text{CF}_3\text{SO}_3)_3$ (Fig. S1, ESI[†]). In the crystal packing, the tricationic complexes are dimerized by π – π interactions between tphz ligands ($d_{\text{tphz-tphz}} = 3.15 \text{ \AA}$, Fig. S2, ESI[†]), and are separated by the triflate counter anions and diethylether lattice molecules.

The presence of a free coordination site on the tphz ligand in **1** prompted us to evaluate the possibility of coordinating another $[(\text{tpy})\text{Cr}]^{3+}$ or $[(\text{tpy})\text{Co}]^{2+}$ moiety on **1**. Unfortunately, this approach was unsuccessful. It seems that when the $[(\text{tpy})\text{Cr}]^{3+}$ moiety is coordinated to one side of tphz, the small Cr^{III} radius together with the tphz rigidity gives rise to a large N4–N6 distance (4.93 Å) at the free coordination site, which no longer fits another small metal ion like Cr^{III} . However, larger metal ions could fit, making this complex a potential switchable building-block for heterometallic architectures.¹¹

Considering the redox-activity of both ligands^{6,7} in the $[(\text{tpy})\text{Cr}^{\text{III}}(\text{tphz})]^{3+}$ cation, the possibility of isolating complexes based on chemically reduced ligands was explored. With one or two equivalents of cobaltocene, the corresponding redox isomers

Table 1 Selected bond distances (Å) at 120 K

	1	1^{red}	1^{redred}
Cr–N1	2.143(6)	2.119(6)	2.126(2)
Cr–N2	1.980(6)	1.900(6)	1.912(2)
Cr–N3	2.122(6)	2.108(6)	2.125(2)
Cr–N7	2.054(6)	2.065(6)	2.039(2)
Cr–N8	1.973(6)	1.998(6)	1.936(2)
Cr–N9	2.050(6)	2.065(6)	2.066(2)
N2...N5	2.772	2.851	2.850
C–C(py _z) ^{ab}	1.403	1.397	1.393
C–N(py _z) ^{ab}	1.342	1.358	1.362
$d_{\text{arom}}(\text{C}_{\text{py}}\text{--}\text{C}_{\text{py}})$ in tpy ^b	1.377	1.377	1.388
$d_{\text{non-arom}}(\text{C}_{\text{py}}\text{--}\text{C}'_{\text{py}})$ in tpy ^b	1.468	1.473	1.449
$d(\text{C}_{\text{py}}\text{--}\text{N}_{\text{py}})$ in tpy ^b	1.349	1.355	1.369

^a pyz = pyrazine part of tphz. ^b Average distance.

$[(\text{tpy})\text{Cr}^{\text{III}}(\text{tphz}^{\bullet-})]^{2+}$ and $[(\text{tpy}^{\bullet-})\text{Cr}^{\text{III}}(\text{tphz}^{\bullet-})]^{+}$ were isolated in $[\text{Cr}^{\text{III}}(\text{tphz}^{\bullet-})(\text{tpy})](\text{CF}_3\text{SO}_3)_2 \cdot \text{CH}_3\text{CN}$ (**1^{red}**, brown needle-shape crystals) and $[\text{Cr}^{\text{III}}(\text{tphz}^{\bullet-})(\text{tpy}^{\bullet-})_2](\text{CF}_3\text{SO}_3)_2 \cdot 3\text{CH}_3\text{CN} \cdot 2\text{Et}_2\text{O}$ (**1^{redred}**, black plate-shape crystals) after the slow diffusion of diethylether in their respective acetonitrile solution (ESI[†]). Both compounds crystallize in the triclinic $P\bar{1}$ space group (Table S1, ESI[†]) and differ by the number of counter anions per cationic unit. Within the three complexes, substantial differences are revealed when comparing the bond distances (Table 1). In particular, upon the first reduction, a significant decrease of the Cr–N2 bond length together with an elongation of the N2...N5 distances in the tphz pyrazine ring constitutes important signatures of the tphz reduction into the radical form, $\text{tphz}^{\bullet-}$.^{6,7} This conclusion is further supported by the absence of significant bond length changes within the tpy ligand, and by X-ray absorption spectroscopy (XAS) at the Cr K-edge of **1** and **1^{red}** (Fig. S3, ESI[†]), which evidences the same +3 oxidation state for the chromium site (see comments in the ESI[†]). Upon the second reduction, the bond distances remain similar for the tphz ligand, whereas noticeable changes are observed for the terpyridine. The increase of the average C–C and C–N bond lengths in the aromatic tpy rings and a shortening of the non-aromatic C–C bonds from *ca.* 1.47 to 1.45 Å (Table 1) are in perfect agreement with the observations made for the reduction of $\text{Cr}^{\text{III}}(\text{tpy})_2^{3+}$ into $\text{Cr}^{\text{III}}(\text{tpy}^{\bullet-})_2^{+}$.¹⁰ The presence of a $\text{tpy}^{\bullet-}$ radical is further supported by characteristic $\pi^* \rightarrow \pi^*$ absorption bands in the NIR region at 973 and 1130 nm, comparable with the spectroscopic signature observed for $\text{Li}(\text{tpy}^{\bullet-})$ (940 nm)¹³ and $\text{Cr}(\text{tpy}^{\bullet-})_2(\text{PF}_6)$ (883 and 1120 nm)¹⁰ (see Fig. S4, ESI[†]). As observed in the crystal packing of **1**, both reduced complexes are dimerized in **1^{red}** and **1^{redred}** by π – π interactions between tphz ligands ($d_{\text{tphz-tphz}} = 3.33$ and 3.25 Å , respectively; Fig. S2, ESI[†]).

The redox-activity of the complexes was also studied by cyclic voltammetry in acetonitrile. Remarkably, not less than six reversible reduction processes were detected for this mononuclear complex, at 0.11, –0.77, –1.21, –1.90, –2.11 and –2.36 V *vs.* Fc^+/Fc (Fig. 2). Each redox process involves one electron, as confirmed by measuring the rest potential of solutions of **1**, **1^{red}** and **1^{redred}**, respectively, at 0.3, –0.1 and –0.8 V *vs.* Fc^+/Fc , prior to recording the cyclic voltammograms, which were found to be identical (Fig. S5, ESI[†]). As discussed previously, combined analyses of bond distances and X-ray absorption spectroscopy allow us to unambiguously assign the two first reductions as being centered on the tphz and tpy ligands, respectively, leading to $[(\text{tpy})\text{Cr}^{\text{III}}(\text{tphz}^{\bullet-})]^{2+}$ and $[(\text{tpy}^{\bullet-})\text{Cr}^{\text{III}}(\text{tphz}^{\bullet-})]^{+}$ species (*vide supra*). These results should be placed in parallel with the rich electrochemistry of $[\text{Cr}(\text{tpy})_2]^{3+}$ reported by Wiegardt *et al.*,¹⁰ who demonstrated that the most accessible four successive reductions are exclusively centered on the tpy ligands. Similarly, one can reasonably assume in the present system that the third and fourth reductions are centered on tphz and tpy, respectively, affording $[(\text{tpy}^{\bullet-})\text{Cr}^{\text{III}}(\text{tphz}^{2-})]$ and $[(\text{tpy}^{2-})\text{Cr}^{\text{III}}(\text{tphz}^{2-})]^{-}$, while the two last reductions are the signature of a third reduction of both ligands at the most negative potentials. However, the use of stronger reducing agents, such as KC_8 , has not allowed us to isolate other more reduced redox isomers so far.

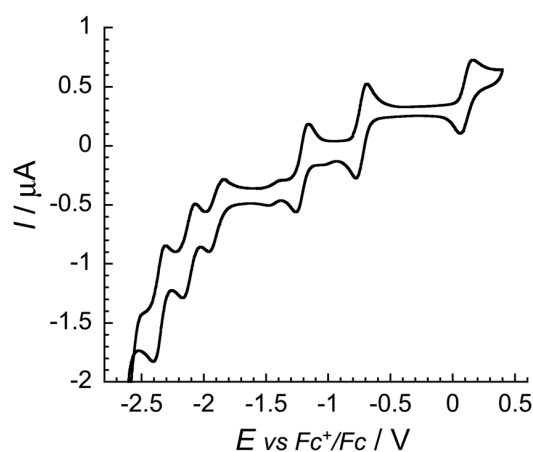


Fig. 2 Cyclic voltammogram for a solution of $\mathbf{1}^{\text{redred}}$ in CH_3CN at a 0.01 V s^{-1} scan rate, and $0.1 \text{ M } (n\text{-Bu}_4\text{N})\text{PF}_6$ as the supporting electrolyte. Further information can be found in the ESI† (Fig. S5).

To probe the strength of the magnetic exchange coupling in these Cr^{III} based complexes and experimentally confirm the key influence of a suitable population of the magnetic 3d orbitals, dc magnetic measurements were performed on polycrystalline samples of the three compounds (ESI†). Above 100 K, the χT products shown in Fig. 3 for the three redox isomers are constant at 1.91 , 1.04 and $0.42 \text{ cm}^3 \text{ K mol}^{-1}$ for $\mathbf{1}$, $\mathbf{1}^{\text{red}}$ and $\mathbf{1}^{\text{redred}}$, respectively, indicating Curie-like behaviors. While for $\mathbf{1}$, the above χT value is expected for a magnetically isolated $S = 3/2 \text{ Cr}^{\text{III}}$ center ($1.875 \text{ cm}^3 \text{ K mol}^{-1}$ for $g = 2$) and consistent with similar mononuclear complexes containing a Cr^{III} metal ion ($g = 2.02$),¹⁴ the results obtained for $\mathbf{1}^{\text{red}}$ and $\mathbf{1}^{\text{redred}}$ are incompatible with a simple Curie constant sum of the involved Cr^{III} and radical spins (2.25 and $2.625 \text{ cm}^3 \text{ K mol}^{-1}$, respectively). This apparent discrepancy is indeed the expected signature of the

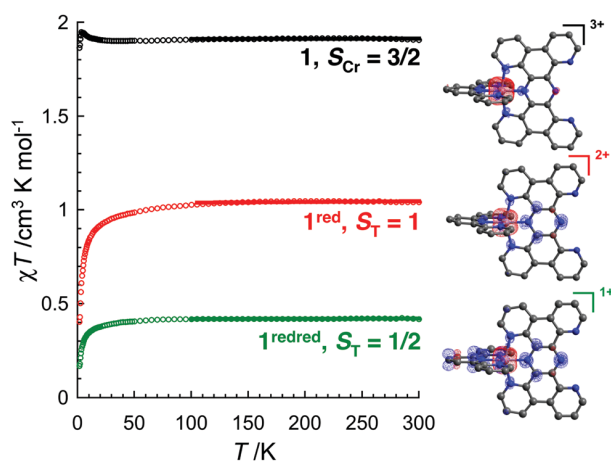


Fig. 3 Temperature dependence of the χT product for $\mathbf{1}$ (black), $\mathbf{1}^{\text{red}}$ (red) and $\mathbf{1}^{\text{redred}}$ (green) at 0.1 T between 1.85 and 40 K and at 1 T above 40 K (χ is defined as the magnetic susceptibility equal to M/H per mole of complex). The solid lines represent the Curie limit at high temperature. Right side: corresponding spin density contour plots (0.005) of a broken-symmetry solution.

extremely large intramolecular magnetic interactions in $\mathbf{1}^{\text{red}}$ and $\mathbf{1}^{\text{redred}}$, separating energetically the spin ground state, S_T , from the excited states, which are not thermally accessible at room temperature. As targeted by selecting the $3d^3$ electronic configuration of the Cr^{III} metal ion, these massive interactions lead to complexes behaving as magnetically isolated S_T macrospins.¹⁵ The χT products above 100 K (1.04 and $0.42 \text{ cm}^3 \text{ K mol}^{-1}$, Fig. 3) for $\mathbf{1}^{\text{red}}$ and $\mathbf{1}^{\text{redred}}$ correspond then to $S_T = 1$ and $S_T = 1/2$ ground states, respectively, as a consequence of huge antiferromagnetic $J_{\text{Cr-tphz}^{\bullet-}}$ and $J_{\text{Cr-tpy}^{\bullet-}}$ exchange couplings. By remaining in the temperature domain below 300 K , at which the complexes are stable, the susceptibility measurements take place in the limit where $J_{\text{Cr-tphz}^{\bullet-}} \gg k_B T$ and $J_{\text{Cr-tpy}^{\bullet-}} \gg k_B T$, and thus these interactions cannot be experimentally determined. On the other hand, a rough estimation of these interactions ($-2J$ formalism) can be obtained from DFT calculations on the basis of the crystal structures: $J_{\text{Cr-tphz}^{\bullet-}}/k_B = -1875$ and -1760 K for $\mathbf{1}^{\text{red}}$ and $\mathbf{1}^{\text{redred}}$, respectively; and $J_{\text{Cr-tpy}^{\bullet-}}/k_B = -1686 \text{ K}$ for $\mathbf{1}^{\text{redred}}$ (cf. Table S2 and comments in Fig. S11 and S12, ESI†). These interaction values place all excited states at more than 5000 K above their respective ground state, which is thus the only thermally populated state at room temperature. As expected for the $3d^3$ configuration, the large $J_{\text{Cr-tphz}^{\bullet-}}$ coupling results from (i) an efficient overlap between the magnetic d_{xy} orbital of the Cr^{III} ion and the $\text{tphz}^{\bullet-} \pi$ system (Fig. S8 and S9, ESI†), as observed for a similar $\text{Co}^{\text{II}}/\text{tphz}$ system,⁶ and (ii) the absence of any antagonist ferromagnetic contribution arising from the population of orthogonal e_g orbitals (as seen in the $\text{Ni}^{\text{II}}/\text{tphz}$ system).⁷ Similarly, a large $J_{\text{Cr-tpy}^{\bullet-}}$ exchange originates from an equally good overlap of the $\pi \text{ tpy}^{\bullet-}$ system with the d_{yz} Cr orbital (Fig. S9, ESI†).‡

Magnetic susceptibility measurements below 100 K (Fig. 3) reveal the presence of weak inter-complex magnetic interactions (ferromagnetic for $\mathbf{1}$ and antiferromagnetic for $\mathbf{1}^{\text{red}}$ and $\mathbf{1}^{\text{redred}}$) likely induced by π - π stacking of the tphz ligand (Fig. S2, ESI†), and/or magnetic anisotropy caused by the distorted octahedral coordination sphere of the $\text{Cr}(\text{III})$ metal ions. These secondary effects are discussed in Fig. S10–S12 (ESI†). Additionally, for the three compounds, it is worth mentioning (i) the absence of the out-of-phase ac susceptibility signal in our experimental window and (ii) the lack of significant luminescence at room temperature in the solid state.

In conclusion, this work illustrates experimentally and theoretically how a suitable population of the magnetic orbitals can be used to rationalize remarkably large exchange couplings. This Cr/tphz system is also a rare example of a complex containing two different ligands, which can be both reduced in a radical form. When doubly reduced, the spin density is fully delocalized on the three components of the complex as depicted in Fig. 3 and Fig. S9 (ESI†). The unpaired electrons of the t_{2g} shell form cubically shaped spin density at the Cr site, whereas the unpaired $\text{tphz}^{\bullet-}$ and $\text{tpy}^{\bullet-}$ electrons are delocalized on π -orbitals of the central pyrazine or pyridine groups, respectively. With the free coordination site of the tphz ligand, this kind of complex could also be used as a switchable magnetic and redox-active module for (supra)molecular architectures with higher dimensionalities or nuclearities.

This work was supported by the ANR (ANR-16-CE29-0001-01, Active-Magnet project), the University of Bordeaux, the Région Nouvelle Aquitaine, the CNRS, the MOLSPIN COST action CA15128 and the CSC for the PhD funding of XM. EAS thanks RSC for the Research Mobility grant and University of Bath HPC facility for computational resources. The authors thank the European Synchrotron Radiation Facility (ESRF, Grenoble, France) for the X-ray spectroscopy experiments and the GdR MCM-2 for fruitful discussions.

‡ As the symmetry around the metal center is not strictly octahedral, the t_{2g} and e_g terms are not strictly accurate either, but they were used as an approximation to facilitate the discussion.

- 1 (a) J. M. Manriquez, G. T. Yee, R. S. McLean, A. J. Epstein and J. S. Miller, *Science*, 1991, **252**, 1415; (b) M. Verdagner, A. Bleuzen, V. Marvaud, J. Vaissermann, M. Seuleiman, C. Desplanches, A. Scullier, C. Train, R. Garde, G. Gelly, C. Lomenech, I. Rosenman, P. Veillet, C. Cartier and F. Villain, *Coord. Chem. Rev.*, 1999, **190–192**, 1023; (c) E. Ruiz, A. Rodriguez-Forteza, S. Alvarez and M. Verdagner, *Chem. – Eur. J.*, 2005, **11**, 2135; (d) H. Phan, T. S. Herg, D. Wang, X. Li, W. Zeng, J. Ding, K. P. Loh, A. T. S. Wee and J. Wu, *Chem*, 2019, **5**, 1.
- 2 M. Gobbi, M. A. Novak and E. Del Barco, *J. Appl. Phys.*, 2019, **125**, 240401.
- 3 (a) C. Coulon, H. Miyasaka and R. Clérac, *Struct. Bonding*, 2006, **122**, 163; (b) W. Zhang, R. Ishikawa, B. Breedlove and M. Yamashita, *RSC Adv.*, 2013, **3**, 3772; (c) C. Coulon, V. Pianet, M. Urdampilleta and R. Clérac, *Struct. Bonding*, 2015, **164**, 143.
- 4 O. Kahn, *Molecular magnetism*, VCH, Weinheim, 1993.
- 5 (a) P. Bonhôte, A. Lecas and E. Amouyal, *Chem. Commun.*, 1998, 885; (b) A. Gourdon and J.-P. Launay, *Inorg. Chem.*, 1998, **37**, 5336.
- 6 X. Ma, E. A. Sutura, S. De, P. Négrier, M. Rouzières, R. Clérac and P. Dechambenoit, *Angew. Chem., Int. Ed.*, 2018, **57**, 7841.
- 7 X. Ma, E. A. Sutura, S. De, M. Rouzières, R. Clérac and P. Dechambenoit, *J. Am. Chem. Soc.*, 2019, **141**(19), 7721.
- 8 The synthesis was made according the procedure reported in the following reference and the crystal structure is reported in ESI†. E. C. Constable, C. E. Housecroft, M. Neuburger, J. Schönle and J. A. Zampese, *Dalton Trans.*, 2014, **43**, 7227.
- 9 I. Brown and D. Altermatt, *Acta Crystallogr., Sect. B: Struct. Sci.*, 1985, **41**, 244.
- 10 C. C. Scarborough, K. M. Lancaster, S. DeBeer, T. Weyhermüller, S. Sproules and K. Wieghardt, *Inorg. Chem.*, 2012, **51**, 3718.
- 11 D. Zare, B. Doistau, H. Nozary, C. Besnard, L. Guénée, Y. Suffren, A.-L. Pelé, A. Hauser and C. Piguet, *Dalton Trans.*, 2017, **46**, 8992.
- 12 S. Otto, M. Grabolle, C. Förster, C. Kreitner, U. Resch-Genger and K. Heinze, *Angew. Chem., Int. Ed.*, 2015, **54**, 11572.
- 13 P. S. Braterman, J. L. Song and R. D. Peacock, *Inorg. Chem.*, 1992, **31**, 555.
- 14 C. C. Scarborough, S. Sproules, T. Weyhermüller, S. DeBeer and K. Wieghardt, *Inorg. Chem.*, 2011, **50**, 12446.
- 15 M. G. Vinum, L. Voigt, C. Bell, D. Mihrin, R. W. Larsen, K. M. Clark and K. S. Pedersen, *Chem. – Eur. J.*, 2020, **26**, 2143.